AIMS Mathematics, 11(2): 4818–4836.
DOI: 10.3934/math.2026197
Received: 07 November 2025
Revised: 07 January 2026
Accepted: 09 January 2026
Published: 27 February 2026

https://www.aimspress.com/journal/Math

*Research article*

# Threshold dynamics in a within-host infection model with Crowley–Martin functional response considering periodic effects

**Ibrahim Nali**[1,*] **and Attila Dénes**[1,2]

[1] Bolyai Institute, University of Szeged, Aradi vértanúk tere 1., H-6720 Szeged, Hungary

[2] National Laboratory for Health Security, Hungary

* **Correspondence:** Email: ibrahimnali@server.math.u-szeged.hu; Tel: +3662546379; Fax: +3662544548.

**Abstract:** In this work, we investigate the threshold dynamics of a within host viral infection model that incorporates a Crowley–Martin functional response together with periodically varying parameters. For this nonautonomous system, we establish the essential analytic properties, namely existence and uniqueness of solutions, positivity, and uniform boundedness of the periodic trajectories. A key component of the analysis is the basic reproduction number $\mathcal{R}_0$, formulated as the spectral radius of an associated integral operator. This quantity acts as the decisive threshold governing the global behavior of the system: if $\mathcal{R}_0 < 1$, all solutions converge to the virus free $\omega$ periodic orbit, whereas $\mathcal{R}_0 > 1$ guarantees uniform persistence and the existence of at least one strictly positive periodic solution. Numerical experiments are provided to illustrate these threshold driven transitions and to complement the theoretical findings.

**Keywords:** within-host virus model; periodic effects; stability analysis; Crowley–Martin functional response
**Mathematics Subject Classification:** 34D05, 92D30

## 1. Introduction

Contemporary studies of infectious diseases increasingly rely on within-host mathematical models to clarify how viruses interact with and influence host cell populations [6]. Such models provide a systematic framework to identify the mechanisms that regulate viral replication, the immune response, and treatment effectiveness, and offer insight into how these mechanisms shape the outcome of an infection. Although many classical models within the host are formulated with constant parameters, It is now well understood that several physiological processes exhibit marked temporal variability [2, 31]. Examples include circadian oscillations in immune activity, periodic dosing in antiviral therapies,

and seasonal variability in within-host dynamics [13, 20, 24]. Incorporating these recurrent influences naturally leads to nonautonomous systems with periodically varying coefficients, and the analysis of such models has revealed a rich array of dynamical behaviors absent in their autonomous counterparts.

The basic reproduction ratio $\mathcal{R}_0$ is a fundamental threshold quantity in the study of infectious disease dynamics. It characterizes the average number of new infections produced by a single infectious individual introduced into a wholly susceptible population. In classical epidemic theory, the interpretation is straightforward: If $\mathcal{R}_0 < 1$, then the infection cannot be sustained and eventually disappears, while $\mathcal{R}_0 > 1$ indicates that the pathogen may persist within the host community. Methods to compute $\mathcal{R}_0$ in autonomous models have been well established [11]. However, when the transmission parameters periodically vary, the determination of $\mathcal{R}_0$ becomes considerably more delicate, as seasonal or treatment-induced fluctuations alter the effective transmission rate [4]. In such settings, relying on an averaged autonomous approximation can lead to misleading conclusions, thus making rigorous definitions of the reproduction ratio essential [14]. Recent developments have provided general frameworks to identify and calculate $\mathcal{R}_0$ in periodic systems [5], and these works demonstrated that it continues to serve as a sharp threshold to govern the stability of the disease-free periodic solution and the global dynamics of infection.

The Crowley–Martin functional response (CMFR) offers a robust framework to model infection dynamics in viral systems by addressing key limitations of bilinear incidence functions. These functions often assume constant interaction rates between host cells and pathogens, an assumption that breaks down in biological scenarios that involve large viral populations due to a competition for resources, thus leading to reduced interaction efficiency [21, 32]. The CMFR, originally developed in the context of predator-prey dynamics, accounts for competition effects and dynamic interaction rates,thus making it particularly suited for in-host models of viral infections [8, 27]. It is defined as follows:

$$\frac{\beta TV}{(1+aT)(1+bV)},$$

where $T$ represents the density of susceptible cells, $V$ denotes the population of free virus particles, $\beta$ is the maximum infection rate, and $a, b > 0$ capture the effects of the capture rate and interference. In this way, the CMFR effectively captures saturation phenomena in viral replication driven by limited target cell availability [7]. Similar to how higher predator densities reduce the feeding rates in predator-prey systems due to spatial factors and competition [9, 10], viral dynamics exhibit similar interference effects, where increasing viral loads diminish the infection efficiency. This refined perspective provides critical insights into the interplay between viruses and immune responses, thus offering a more biologically realistic depiction of in-host viral dynamics.

The present work extends an autonomous within-host viral infection model previously studied in the context of the Usutu virus [26] to a non-autonomous setting with periodic coefficients. While Usutu virus provides the original biological motivation for the model structure, the focus here is on the general mathematical effects of periodicity on the within-host dynamics. Although environmental factors such as climatic variability and vector dynamics are known to influence viral transmission at the population level [18,19,23], it is equally important to account for periodic effects that act within the host, including physiological rhythms and time-dependent treatment processes [3, 15, 22, 32]. Seasonal or circadian variations in immune activity, as well as the timing of repeated therapeutic interventions, can significantly affect the viral replication and clearance rates. Motivated by these considerations, we

incorporate periodic coefficients together with a CMFR, thus enabling a general and flexible framework to investigate how time-dependent host factors shape the within-host viral dynamics.

Building on this framework, the present work develops a within-host viral infection model with periodically varying parameters, aimed at capturing recurrent biological influences on the infection dynamics in a general setting. Our main objective is to understand how the long-term behavior of the system is governed by the basic reproduction number $\mathcal{R}_0$, which is defined via the spectral radius of an associated integral operator. Within this framework, we establish fundamental mathematical properties of the model, including the existence and uniqueness of solutions, positivity, and uniform boundedness for all time. We further show that the virus-free periodic solution is globally asymptotically stable when $\mathcal{R}_0 < 1$, whereas the case $\mathcal{R}_0 > 1$ leads to uniform persistence of the infection and guarantees the existence of at least one positive periodic solution. To complement the theoretical analysis, we also present numerical simulations that illustrate the threshold behavior and highlight the influence of periodic forcing on the system's dynamics.

## 2. Model derivation

Following the modeling perspective of Heitzman-Breen et al. [17], we construct a system that incorporates a CMFR to reflect saturation effects in the infection pathway. The total population of host cells is separated into three compartments:

- **Target cells ($T$):** Susceptible cells available for viral infection.
- **Exposed cells ($E$):** Newly infected cells that have entered the latent stage.
- **Infected cells ($I$):** Productively infected cells contributing to viral replication.

Additionally, the dynamics of free virus particles ($V$) are explicitly modeled. To account for key processes within the host, time-dependent parameters are introduced to represent periodic influences that arise from environmental, physiological, or therapeutic factors.

In addition to the cellular compartments, we also model the population of free virus particles, denoted by $V(t)$. Several parameters that govern the within-host dynamics are assumed to vary periodically vary in time to capture recurrent physiological or external influences. In particular, new target cells enter the system according to a time-dependent production function $\mu(t)$, while they are removed at a clearance rate $d(t)$. Both functions are taken to be bounded, continuous, and $\omega$-periodic, thus reflecting rhythmic biological patterns such as circadian or seasonal fluctuations that may affect the availability of susceptible cells. The transmission coefficient $\beta(t)$ is likewise modeled as an $\omega$-periodic function to represent time-dependent variations in the infection efficiency that may arise from changes in the immune activity or other host-related factors. The remaining parameters describe intrinsic biological processes that are assumed to slowly vary; and are therefore treated as constants over the time scale considered.

The interaction between target cells and the virus is described through a CMFR,

$$\frac{\beta(t)\, T\, V}{(1+\alpha_1 T)\,(1+\alpha_2 V)},$$

which incorporates the saturation effects due to competition among virus particles and limited access to susceptible cells.

Thus, the model is governed by the following differential system:

$$\begin{aligned}
\frac{dT}{dt} &= \mu(t) - \frac{\beta(t)TV}{(1+\alpha_1 T)(1+\alpha_2 V)} - d(t)T,\\
\frac{dE}{dt} &= \frac{\beta(t)TV}{(1+\alpha_1 T)(1+\alpha_2 V)} - kE - d(t)E,\\
\frac{dI}{dt} &= kE - \delta I - d(t)I,\\
\frac{dV}{dt} &= pI - cV.
\end{aligned} \tag{2.1}$$

A summary of the model parameters and their biological interpretations is given in Table 1.

**Table 1.** Model parameters.

| Parameter | Definition |
|---|---|
| $\mu(t)$ | $\omega$-periodic production rate of target cells |
| $d(t)$ | $\omega$-periodic clearance rate of target cells |
| $\beta(t)$ | $\omega$-periodic infection transmission rate |
| $k$ | Transition rate from exposed to infectious cells |
| $\delta$ | Death rate of infected cells due to viral damage |
| $p$ | Viral production rate per infected cell |
| $c$ | Clearance rate of free virus particles |
| $\alpha_1$ | Saturation parameter associated with target cells |
| $\alpha_2$ | Saturation parameter associated with virus concentration |

The present non-autonomous model is an extension of previously studied autonomous within-host models motivated by the Usutu virus dynamics [17,26]. As emphasized in the autonomous setting, the underlying model structure is not specific to the Usutu virus. By incorporating periodic coefficients, this time-dependent formulation extends the original time-constant model [26] and provides a flexible framework to analyze infection dynamics under more realistic conditions. In particular, the inclusion of periodic parameters allows the model to capture oscillatory behaviors that arise from external and internal influences, such as seasonal variability or periodic therapeutic interventions.

## 3. Qualitative properties of the model

We begin with an examination of the qualitative behavior of system (2.1). In particular, we establish that solutions remain positive and uniformly bounded for all forward time, thus ensuring that the system is mathematically well posed.

**Lemma 1.** *Let* $(T(0), E(0), I(0), V(0)) \in \mathbb{R}^4_+$. *Then, the corresponding solution of system* (2.1) *satisfies*

$$T(t), E(t), I(t), V(t) > 0 \quad \textit{for all } t > 0,$$

*and there exists a constant* $M > 0$ *such that*

$$T(t),\ E(t),\ I(t),\ V(t) \le M \quad \textit{for all } t \ge 0.$$

*Proof.* Let $\kappa$ be defined as $\kappa = \sup\{t > 0 : T(t) > 0, E(t) > 0, I(t) > 0, V(t) > 0\}$. It is evident that $\kappa > 0$. Now, consider the following scenarios: either $\kappa = \infty$ or $\kappa < \infty$. In the former case, the solutions trivially remain positive. In the latter case, let us assume the opposite, (i.e, at least one of $T(\kappa)$, $E(\kappa)$, $I(\kappa)$, or $V(\kappa)$ is zero).

From system (2.1), we obtain

$$\begin{aligned}
\frac{dT}{dt} &\geq -\frac{\beta(t)TV}{(1+\alpha_1 T)(1+\alpha_2 V)} - d(t)T,\\
\frac{dE}{dt} &\geq -kE - d(t)E,\\
\frac{dI}{dt} &\geq -\delta I - d(t)I,\\
\frac{dV}{dt} &\geq -cV,
\end{aligned}$$

which imply the estimates

$$\begin{aligned}
T(\kappa) &\geq T_0 \exp\left\{-\int_0^{\kappa}\left(\frac{\beta(u)V(u)}{(1+\alpha_1 T(u))(1+\alpha_2 V(u))} - d(u)\right) du\right\} > 0,\\
E(\kappa) &\geq E_0 \exp\left\{-\int_0^{\kappa}(k + d(u))\, du\right\} > 0,\\
I(\kappa) &\geq I_0 \exp\left\{-\int_0^{\kappa}\delta + d(u)\, du\right\} > 0,\\
V(\kappa) &\geq V_0 \exp\{-c\kappa\} > 0.
\end{aligned}$$

Thus, $T(\kappa) > 0$, $E(\kappa) > 0$, $I(\kappa) > 0$, and $V(\kappa) > 0 \Rightarrow T(t) > 0$, $E(t) > 0$, $I(t) > 0$, and $V(t) > 0$ for any $t > 0$. This contradicts our assumption that $T(\kappa) = 0$, $E(\kappa)$, $I(\kappa)$, and $V(\kappa) = 0$. Therefore, $T(t) > 0$, $E(t) > 0$, $I(t) > 0$, and $V(t) > 0$, for all $t > 0$.

Our next goal is to demonstrate that the solutions of the system remain bounded. Consider the quantity $W(t) = T(t) + E(t) + I(t) + \frac{\delta+d(t)}{2p}V(t)$. The derivative of $W$ can be computed as follows:

$$\begin{aligned}
\dot{W} &= \dot{T} + \dot{E} + \dot{I} + \frac{\delta + d(t)}{2p}\dot{V}\\
&= \mu(t) - d(t)T - d(t)E - \frac{\delta + d(t)}{2}I - cV\\
&\leq \mu(t) - m\left(T + E + I + \frac{\delta + d(t)}{2p}V\right) \leq \zeta - mW,
\end{aligned}$$

where $\zeta = \max_{t\in[0,T_M)}\mu(t)$, and $m$ is defined as $m = \min\{\min_{t\in[0,T_M)}, \min_{t\in[0,T_M)}\frac{\delta+d(t)}{2p}, c\}$. The inequality can be rewritten as $\dot{W} + mW \leq \zeta$, which forms a linear ordinary differential inequality with a negative coefficient for $W$. By applying the integrating factor $e^{mt}$, we obtain the following:

$$W(t) \leq e^{-mt}\left(W(0) - \frac{\zeta}{m}\right) + \frac{\zeta}{m}.$$

This implies that $0 \leq W(t) \leq \xi$, where $\xi = \frac{\zeta}{m}$. Consequently, we have $0 \leq T(t), E(t), I(t) \leq \xi$, and $0 \leq V(t) \leq N_1$ for all $t \geq 0$, provided that the initial conditions satisfy $T(0)+E(0)+I(0)+\frac{\delta+d(0)}{2p}V(0) \leq \xi$.

Here, we define $N_1 = \frac{2p\xi}{\delta+D}$. In summary, we have successfully demonstrated that the solutions are bounded. Therefore, we can state that the set

$$\mathcal{D} := \left\{(T, E, I, V) \in \mathbb{R}^4_+ \mid T + E + I \leq 3\xi,\ V \leq N_1\right\}$$

is a positively invariant, compact, and attractor. □

## 4. Existence and uniqueness of the virus-free $\omega$-periodic solution

**Lemma 2.** *There exists exactly one virus-free solution of system* (2.1) *that is $\omega$-periodic. It has the form*

$$\mathcal{E}_0 = (T^*(t), 0, 0, 0),$$

*with $T^*(t)$ being the unique $\omega$-periodic solution of* (4.1).

*Proof.* From system (2.1), by setting $V = 0$, we have the following equation:

$$\frac{dT}{dt} = \mu(t) - d(t)T \tag{4.1}$$

with the initial condition $T(0) = T_0 \in \mathbb{R}_+$.

From (4.1), we have the following

$$\frac{dT}{dt} + d(t)T = \mu(t).$$

Multiplying by $e^{\int_0^t d(\xi)d\xi}$, we have the following:

$$\frac{dT}{dt}e^{\int_0^t d(\xi)d\xi} + d(t)Te^{\int_0^t d(\xi)d\xi} = \mu(t)e^{\int_0^t d(\xi)d\xi}.$$

After integrating both sides, we obtain the following

$$T(t) = e^{-\int_0^t d(\xi)d\xi}\left(\int_0^t \mu(\tau)e^{\int_0^\tau d(\xi)d\xi} + T_0\right).$$

To find the virus-free periodic solution $T^*(t)$, we must ensure $T^*(t+\omega) = T^*(t)$; from this, one gets the $\omega$-periodic solution as follows:

$$T^*(t) = e^{-\int_0^t d(\xi)d\xi}\left(\int_0^t \mu(\tau)e^{\int_0^\tau d(\xi)d\xi} + \frac{e^{-\int_0^\omega d(\xi)d\xi}\int_0^\omega \mu(\tau)e^{\int_0^\tau d(\xi)d\xi}d\tau}{1 - e^{-\int_0^\omega d(\xi)d\xi}}\right).$$

□

## 5. The basic reproduction ratio

The preceding section introduced the heterogeneous epidemiological model under periodic forcing. The next step of the analysis is to determine the basic reproduction ratio $\mathcal{R}_0$ and to examine the stability characteristics of the virus-free equilibrium. To calculate $\mathcal{R}_0$, we employ the technique outlined in [30].

Subsequently, we extend our investigation to assess the stability of the periodic virus-free steady state, thereby utilizing the same methodology.

We define $\mathcal{F}(t,x)$ as the input rate of newly infected individuals in the $i$-th compartment, $\mathcal{V}^+(t,x)$ as the input rate of individuals through other means, and $\mathcal{V}^-(t,x)$ as the rate of transfer of individuals out of compartment $i$. Specifically,

$$\mathcal{F}(t,x) = \begin{bmatrix} \frac{\beta(t)TV}{(1+\alpha_1 T)(1+\alpha_2 V)} \\ 0 \\ 0 \\ 0 \end{bmatrix},$$

$$\mathcal{V}^+(t,x) = \begin{bmatrix} 0 \\ kE \\ pI \\ \mu(t) \end{bmatrix}, \qquad \mathcal{V}^-(t,x) = \begin{bmatrix} (k+d(t))E \\ (\delta+d(t))I \\ cV \\ \frac{\beta(t)TV}{(1+\alpha_1 T)(1+\alpha_2 V)} + d(t)T \end{bmatrix}.$$

Let us introduce the vector variable $x = (E, I, V, T)$, where the first three components correspond to the infection-related classes, and $T$ denotes the susceptible cell population. Following the notation of [30], system (2.1) may be expressed in the following general form:

$$\frac{dx_i}{dt} = \mathcal{F}_i(t,x) - (\mathcal{V}_i^-(t,x) - \mathcal{V}_i^+(t,x)) \equiv f_i(t,x), \qquad i = 1,\dots,4.$$

One can directly verify that system (2.1) satisfies the structural conditions (A1)–(A5) stated in [30].

Let $x^* = (0,0,0,T^*(t))$ denote the virus-free $\omega$-periodic solution of system (2.1), where $T^*(t)$ is the unique $\omega$-periodic solution of the scalar equation (4.1). We define the following:

$$F(t) = \left(\frac{\partial \mathcal{F}_i(t,x^*)}{\partial x_j}\right)_{1\le i,j\le 3} = \begin{bmatrix} 0 & 0 & \beta(t)\frac{T^*(t)}{1+\alpha_1 T^*(t)} \\ 0 & 0 & 0 \\ 0 & 0 & 0 \end{bmatrix},$$

$$G(t) = \left(\frac{\partial \mathcal{V}_i(t,x^*)}{\partial x_j}\right)_{1\le i,j\le 3} = \begin{bmatrix} \kappa + d(t) & 0 & 0 \\ -\kappa & \delta + d(t) & 0 \\ 0 & -p & c \end{bmatrix}.$$

Let $\Phi_M(t)$ and $\rho(\Phi_M(\omega))$ be the monodromy matrix of the linear $\omega$-periodic system $\frac{dz(t)}{dt} = M(t)z$ and the spectral radius of $\Phi_M(\omega)$. In order to apply the operator theoretic framework in [30], we assume that the virus-free $\omega$-periodic solution is linearly asymptotically stable in the virus-free subspace. More precisely, we impose the following condition:

**(A6)** $\rho(\Phi_M(\omega)) < 1$.

Next, let $X(t,s), t \ge s$, be the evolution operator of the linear $\omega$-periodic system

$$\frac{dy}{dt} = -G(t)y,$$

that is, for each $s \in \mathbb{R}$, the $3 \times 3$ matrix $X(t, s)$ satisfies the following:

$$\frac{dX(t,s)}{dt} = -G(t)X(t,s), \quad \forall t \geq s, \quad X(s,s) = I,$$

where $I$ is the $3 \times 3$ identity matrix. Thus, the monodromy matrix $\Phi_{-G}(t)$ of system (5.1) equals to $X(t, 0),\ t \geq 0$.

We assume that

**(A7)** $\rho(\Phi_{-G}(\omega)) < 1$.

Assumption **(A7)** ensures that the infected compartments decay exponentially over time in the qbsence of new infections. In particular, by the standard theory of linear periodic systems, there exist constants $K > 0$ and $\alpha > 0$ such that the evolution operator $X(t, s)$ of $\dot{y} = -G(t)y$ satisfies the following:

$$\|X(t,s)\| \leq Ke^{-\alpha(t-s)}, \qquad \forall\, t \geq s.$$

Based on the aforementioned assumptions, we are now in a position to analyze the basic reproduction ratio of our model (2.1) by tracking the cumulative contribution of newly infected individuals over time.

Let $\psi(s)$ denote the distribution of infected individuals, which exhibits $\omega$-periodicity in $s$. The expression $F(s)\psi(s)$ signifies the rate of new cases that arise from individuals infected at time $s$. Beyond this, for $t \geq s$, the term $X(t, s)F(s)\psi(s)$ characterizes the distribution of individuals who contracted the infection at time $s$ and remain infectious at time $t$. Consequently,

$$g(t) := \int_{-\infty}^{t} X(t,s)F(s)\psi(s)ds = \int_{0}^{\infty} X(t,t-a)F(t-a)\psi(t-a)da. \tag{5.1}$$

Function $g(t)$ represents the distribution of cumulative new infections at time $t$, which is generated by all infected individuals $\psi(s)$ introduced at any time $s \leq t$.

Let us denote the ordered Banach space of $\omega$-periodic functions acting from $\mathbb{R}$ to $\mathbb{R}^6$ by $C_\omega$, which is equipped with the maximum norm $\|\cdot\|_\infty$, and let us introduce the positive cone as follows:

$$C_\omega^+ := \{\psi \in C_\omega : \psi(t) \geq 0, \forall t \in \mathbb{R}\}. \tag{5.2}$$

In the following, we define the linear next infection operator $L\colon C_\omega \to C_\omega$ as follows:

$$(L\psi)(t) = \int_{0}^{\infty} X(t,t-a)F(t-a)\psi(t-a)da, \quad \forall t \in \mathbb{R}, \psi \in C_\omega. \tag{5.3}$$

The basic reproduction ratio associated with system (2.1) is introduced as follows:

$$\mathcal{R}_0 := \rho(L),$$

where $\rho(L)$ denotes the spectral radius of the corresponding next–generation operator $L$. In the autonomous setting, the expression obtained in [26] takes the explicit form as follows

$$\mathcal{R}_0 = \frac{p\,\beta\,k\,\mu}{c\,(d+\delta)(d+k)\,(d+\alpha_1\mu)}.$$

Furthermore, consider the following linear $\omega$-periodic system:

$$\frac{dw(t)}{dt} = \left(\frac{1}{\lambda}F(t) - G(t)\right)w(t), \qquad t \in \mathbb{R}. \tag{5.4}$$

Let $W(t, s, \lambda)$, $t \geq s$, denote the evolution operator of this system on $\mathbb{R}^3$. By construction, for $\lambda = 1$, we have the following

$$W(t, 0, 1) = \Phi_{F-G}(t), \qquad \forall\, t \geq 0,$$

where $\Phi_{F-G}(t)$ is the fundamental solution matrix of the linearized infected subsystem.

Since $F(t)$ is nonnegative and $-G(t)$ is cooperative, the system above is cooperative for each $\lambda > 0$, and hence $W(t, s, \lambda)$ is a positive operator. Moreover, due to $\omega$-periodicity, the monodromy matrices $W(s + \omega, s, \lambda)$ and $W(\omega, 0, \lambda)$ are similar for all $s \in \mathbb{R}$ and therefore have the same spectrum.

Under Assumption **(A7)**, the linear system $\frac{dy}{dt} = -G(t)y$, is uniformly exponentially stable, which guarantees that the next infection operator $L$ is well defined and bounded on $C_\omega$. In this framework, the basic reproduction ratio $\mathcal{R}_0 = \rho(L)$ admits the following characterization: if there exists $\lambda_0 > 0$ such that

$$\rho(W(\omega, 0, \lambda_0)) = 1,$$

then $\lambda_0$ is an eigenvalue of $L$ and hence $\mathcal{R}_0 > 0$. Conversely, if $\mathcal{R}_0 > 0$, then $\lambda = \mathcal{R}_0$ is the unique positive solution of $\rho(W(\omega, 0, \lambda)) = 1$. Furthermore, $\mathcal{R}_0 = 0$ if and only if $\rho(W(\omega, 0, \lambda)) < 1$ for all $\lambda > 0$.

This value of $\lambda_0$ can be numerically evaluated via the associated spectral radius.

## 6. Stability analysis

The stability of the virus-free periodic orbit $\mathcal{E}_0$ is determined by examining the spectral properties of the linearized evolution operator. A key result from [30], together with a supporting lemma from [25], provides the threshold conditions that relate $\mathcal{R}_0$ to the spectrum of $\Phi_{F-V}(\omega)$.

**Theorem 1** ([30, Theorem 2.2])**.** *The following equivalences hold for system* (2.1)*:*

*(i)* $\mathcal{R}_0 = 1$ *is equivalent to* $\rho(\Phi_{F-V}(\omega)) = 1$,
*(ii)* $\mathcal{R}_0 > 1$ *is equivalent to* $\rho(\Phi_{F-V}(\omega)) > 1$, *and*
*(iii)* $\mathcal{R}_0 < 1$ *is equivalent to* $\rho(\Phi_{F-V}(\omega)) < 1$.

**Lemma 3.** *Consider a matrix function $A(t)$ that is continuous, irreducible, cooperative, and $\omega$-periodic. The corresponding linear variational system*

$$x' = A(t)x \tag{6.1}$$

*admits a fundamental matrix solution, which we denote by $\Phi_A(t)$.*

*Define the following:*

$$\sigma = \frac{1}{\omega}\ln(\rho(\Phi_A(\omega))),$$

*where the notation $\rho(\cdot)$ is used for the spectral radius. Then there exists a strictly positive $\omega$-periodic function $v(t)$ for which the function $e^{\sigma t}v(t)$ satisfies linear equation* (6.1).

*6.1. Local and global stability of the virus-free periodic solution*

**Theorem 2.** *If $\mathcal{R}_0 < 1$, then the virus-free periodic solution $\mathcal{E}_0$ is both locally and globally asymptotically stable in $\mathbb{R}^4_+$.*

*Proof.* To verify the local asymptotic stability of the virus-free periodic state $\mathcal{E}_0$ under the condition $\mathcal{R}_0 < 1$, we make use of two key results presented in [30]. Beyond the local behavior, it remains necessary to demonstrate that $\mathcal{E}_0$ attracts all trajectories in $\mathbb{R}^3_+$ when $\mathcal{R}_0 < 1$, thereby thus establishing its global attractiveness.

By Lemma 2, given any $\epsilon > 0$ there exists a time $T_1 > 0$ such that

$$T(t) \leq T^*(t) + \epsilon \qquad \text{for all } t > T_1.$$

The function $f(x) = \frac{x}{1+cx}$ is monotone increasing on $\mathbb{R}$, and therefore we obtain the following:

$$\frac{\beta(t)T(t)V(t)}{(1+\alpha_1 T(t))(1+\alpha_2 V(t))} \leq \frac{\beta(t)T(t)}{1+\alpha_1 T(t)} \leq \beta(t)\frac{T^*(t)+\epsilon}{1+CT^*(t)},$$

for $t > T_1$. Consequently, from system (2.1), we obtain

$$\begin{cases} E' \leq \beta(t)\frac{T^*(t)+\epsilon}{1+CT^*(t)} - (k+d(t))E, \\ I' = kE - (\delta + d(t))I, \\ V' = pI - cV. \end{cases}$$

Define the following matrix:

$$M_1(t) = \begin{bmatrix} 0 & 0 & \beta(t) \\ 0 & 0 & 0 \\ 0 & 0 & 0 \end{bmatrix}.$$

Using Theorem 1, we deduce that $\rho\left(\Phi_{F-G}(\omega)\right) < 1$. Select $\epsilon > 0$ such that $\rho\left(\Phi_{F-G+\varphi(\epsilon)M_1}(\omega)\right) < 1$, and consider the following modified system:

$$\begin{bmatrix} \bar{E}' \\ \bar{I}' \\ \bar{V}' \end{bmatrix} = (F(t) - G(t) + \varphi(\epsilon)M_1(t)) \begin{bmatrix} \bar{E} \\ \bar{I} \\ \bar{V} \end{bmatrix}.$$

Invoking Lemma 3 and applying the comparison principle, we find $\omega$-periodic functions $v_1(t)$, $v_2(t)$ and $v_3(t)$ such that

$$E(t) \leq v_1(t)e^{\sigma t}, \quad I(t) \leq v_2(t)e^{\sigma t}, \quad \text{and} \quad V(t) \leq v_3(t)e^{\sigma t},$$

where $\sigma = \frac{1}{\omega}\ln\left(\rho(\Phi_{F-G+\varphi(\epsilon)M_1}(\omega))\right)$. This implies that $E(t) \to 0$, $I(t) \to 0$, and $V(t) \to 0$ as $t \to \infty$.

Therefore, we have the following:

$$\lim_{t\to\infty}\left(T(t) - T^*(t)\right) = 0.$$

The proof is now complete. □

*6.2. Persistence of the infective compartment and existence of endemic periodic orbits*

Let $u(t, X_0)$ denote the solution of system (2.1) with the initial condition $X_0 = (T^0, E^0, I^0, V^0) \in \mathbb{R}^4_+$. The right-hand side of system (2.1) is continuous with respect to $t$ and locally Lipschitz continuous with respect to the state variables $(T, E, I, V)$ on $\mathbb{R}^4_+$. Therefore, by the classical existence–uniqueness theorem for ordinary differential equations [28], system (2.1) admits a unique local solution. Furthermore, the uniform boundedness established in Lemma 1 guarantees that this solution can be globally extended, and hence the solution exists for all $t \geq 0$. In particular, for any initial condition $X_0 \in \text{int}(\mathbb{R}^4_+)$, the solution remains strictly positive for all $t > 0$.

Define the Poincaré map $Q\colon \mathbb{R}^4_+ \to \mathbb{R}^4_+$ associated with system (2.1) as $Q(X_0) = u(\omega, X_0)$ for all $X_0 \in \mathbb{R}^4_+$. Consider the set $\Gamma = \left\{(T, E, I, V) \in \mathbb{R}^4_+\right\}$, its interior $\Gamma_0 = \text{Int}(\mathbb{R}^4_+)$, and its boundary $\partial\Gamma_0 = \Gamma \setminus \Gamma_0$. Note that both $\Gamma$ and $\Gamma_0$ are positively invariant under the dynamics of the system, and that $Q$ is point dissipative.

Now, define the following set:

$$M_\partial = \left\{\left(T^0, E^0, I^0, V^0\right) \in \partial\Gamma_0 : Q^n\left(T^0, E^0, I^0, V^0\right) \in \partial\Gamma_0, \text{ for all } n \geq 0\right\}.$$

In order to invoke the uniform persistence framework developed in [33], it remains to verify that

$$M_\partial = \left\{(T, 0, 0, 0) \in \mathbb{R}^4_+ : T \geq 0\right\}. \tag{6.2}$$

Note that $M_\partial \supseteq \{(T, 0, 0, 0) \in \mathbb{R}^4_+ : T \geq 0\}$, to show that $M_\partial \subseteq \{(T, 0, 0, 0) \in \mathbb{R}^4_+ : T \geq 0\}$. We begin by using a contradiction argument. Assume that $M_\partial$ is not a subset of $\{(T, 0, 0, 0) \in \mathbb{R}^4_+ : T \geq 0\}$. This implies that there exists an initial condition $(T(0), E(0), I(0), V(0)) \in \partial\Gamma_0$ such that for some $m_1 \geq 0$, the solution satisfies $(E(m_1\omega), I(m_1\omega), V(m_1\omega))^T > 0$.

Now, consider $m_1\omega$ as the initial time. From the positivity of the solutions discussed earlier, we have $(T(t), E(t), I(t), V(t)) > 0$ for all $t > m_1\omega$. This implies that $(T(t), E(t), I(t), V(t)) \in \Gamma_0$ for all $t > m_1\omega$, meaning the solution enters the interior of $\Gamma$, which contradicts the assumption that it remains on $\partial\Gamma_0$.

Thus, our assumption must be false, and we therefore obtain $M_\partial \subseteq \{(T, 0, 0, 0) \in \mathbb{R}^4_+ : T \geq 0\}$, thereby thus proving that equality (6.2) holds. Therefore, we can conclude that the disease is uniformly persistent, as stated below.

**Theorem 3.** *Suppose that $\mathcal{R}_0 > 1$. Then, system* (2.1) *has at least one positive periodic solution. Moreover, there exists a constant $\eta > 0$ such that for any initial condition $\left(T^0, E^0, I^0, V^0\right) \in \Gamma_0$, we have the following:*

$$\liminf_{t\to\infty}(E(t), I(t), V(t)) \geq (\eta, \eta, \eta).$$

*Proof.* The proof follows a similar approach to that presented in [1, 12]. We start by proving that the trajectory of (2.1) is uniformly persistent w.r.t. $(\Gamma_0, \partial\Gamma_0)$ by applying (Theorem 3.1.1 in [33]). Let us recall that Theorem 1 implies $\rho(\varphi_{F-G}(T)) > 1$. Therefore, there exists $\nu > 0$ small enough that satisfies $r(\varphi_{F-G-\nu M_1}(T)) > 1$. Let us consider the following perturbed equation:

$$\frac{dT_\alpha}{dt} = \mu(t) - \alpha\frac{\beta(t)T_\alpha}{(1 + \alpha_1 T_\alpha)(1 + \alpha_2\alpha)} - d(t)T_\alpha. \tag{6.3}$$

The function $Q$ associated with (6.3) has a unique positive fixed point $\left(\bar{T}_{\alpha}^{0}\right)$ that it is globally attractive in $\mathbb{R}_{+}$. We apply the implicit function theorem to obtain the continuity of $\left(\bar{T}_{\alpha}^{0}\right)$ with respect to $\alpha$. Therefore, we can choose $\alpha > 0$ small enough that satisfies $\bar{T}_{\alpha}(t) > \bar{T}(t) - \nu$ for all $t > 0$. Let $M_1 = \left(\bar{T}^0, 0, 0, 0\right)$. Since the trajectory is continuous with respect to the initial condition, there exists $\alpha^*$ that satisfies $\left(T^0, E^0, I^0, V^0\right) \in \Gamma_0$ with $\| \left(T^0, E^0, I^0, V^0\right) - u\left(t, M_1\right) \| \leq \alpha^*$; it holds that

$$\left\| u\left(t, \left(T^0, E^0, I^0, V^0\right)\right) - u\left(t, M_1\right) \right\| < \alpha \quad \text{for } 0 \leq t \leq T.$$

By contradiction, we can show the following:

$$\limsup_{n\to\infty} d\left(P^n\left(T^0, E^0, I^0, V^0\right), M_1\right) \geq \alpha^* \qquad \forall \left(T^0, E^0, I^0, V^0\right) \in \Gamma_0. \tag{6.4}$$

Suppose that $\limsup_{n\to\infty} d\left(Q^n\left(T^0, E^0, I^0, V^0\right), M_1\right) < \alpha^*$ for some $\left(T^0, E^0, I^0, V^0\right) \in \Gamma_0$. We can assume that $d\left(Q^n\left(T^0, E^0, I^0, V^0\right), M_1\right) < \alpha^*$ for all $n > 0$. Therefore,

$$\left\| u\left(t, Q^n\left(T^0, E^0, I^0, V^0\right)\right) - u\left(t, M_1\right) \right\| < \alpha \qquad \forall n > 0 \text{ and } 0 \leq t \leq \omega.$$

For all $t \geq 0$, let $t = n\omega + t_1$, with $t_1 \in [0, \omega)$ and $n = \left[\frac{t}{\omega}\right]$ (i.e, the greatest integer $\leq \frac{t}{\omega}$). Then, we obtain the following:

$$\left\| u\left(t, \left(T^0, E^0, I^0, V^0\right)\right) - u\left(t, M_1\right) \right\| = \left\| u\left(t_1, P^n\left(T^0, E^0, I^0, V^0\right)\right) - u\left(t_1, M_1\right) \right\| < \alpha \quad \text{for all } t \geq 0.$$

Set $(T(t), E(t), I(t), V(t)) = u\left(t, \left(T^0, E^0, I^0, V^0\right)\right)$. Therefore, $0 \leq E(t), I(t), V(t) \leq \alpha, t \geq 0$ and □

$$\frac{dT_{\alpha}}{dt} \geq \mu(t) - \alpha \frac{\beta(t)T}{(1+\alpha_1 T)(1+\alpha_2 \alpha)} - d(t)T. \tag{6.5}$$

The fixed point $\bar{T}_{\alpha}^{0}$ of the function $Q$ associated with (6.3) is globally attractive such that $\bar{T}_{\alpha}(t) > \bar{T}(t) - \nu$; then, there exists $T_2 > 0$ large enough that satisfies $T(t) > \bar{T}(t) - \nu$. Therefore, for $t > T_2$,

$$\begin{cases} \dfrac{dE}{dt} \geq \dfrac{\beta(t)(\bar{T}(t) - \nu)V}{(1 + \alpha_1(\bar{T}(t) - \nu))(1 + \alpha_2 V)} - kE - d(t)E, \\ \dfrac{dI}{dt} = kE - \delta I - d(t)I, \\ \dfrac{dV}{dt} = pI - cV. \end{cases}$$

Note that we have the condition that $\rho\left(\varphi_{F-G-\nu M_2}(\omega)\right) > 1$. Lemma 3 and the comparison principle together imply the existence of a positive $\omega$-periodic trajectory $y_2(t)$ that satisfies $J(t) \geq e^{k_2 t} y_2(t)$ with $k_2 = \frac{1}{\omega} \ln \rho\left(\varphi_{F-G-\nu M_2}(\omega)\right) > 0$, which further implies $\lim_{t\to\infty} E(t) = \infty$, $\lim_{t\to\infty} I(t) = \infty$ and $\lim_{t\to\infty} V(t) = \infty$ which cannot hold as trajectories that are bounded. Hence, (6.4) is satisfied and we obtain the weak uniform persistence of $Q$ w.r.t. $(\Gamma_0, \partial\Gamma_0)$. Lemma 1 implies that $P$ has a global attractor; then, we obtain that $M_1$ is an isolated invariant set in $X$ and $W^s(M_1) \cap \Gamma_0 = \emptyset$. Clearly, each solution in $M_\partial$ converges to $M_1$ and $M_1$ is acyclic in $M_\partial$. From (Theorem 1.3.1 and Remark 1.3.1 in [33]), we

obtain that $Q$ is uniformly persistent with respect to $(\Gamma_0, \partial\Gamma_0)$. Moreover, according to (Theorem 1.3.6 in [33]), $Q$ has a fixed point $\left(\tilde{T}^0, \tilde{E}^0, \tilde{I}^0, \tilde{V}^0\right) \in \Gamma_0$. We can see that

$$\left(\tilde{T}^0, \tilde{E}^0, \tilde{I}^0, \tilde{V}^0\right) \in R_+ \times \mathrm{Int}\left(R_+^3\right).$$

To show that $\tilde{T}^0 > 0$, we will again argue by contradiction. Suppose $\tilde{T}^0 = 0$. The first equation of (2.1) verifies that

$$\dot{\tilde{T}}(t) \geq \mu(t) - \frac{\beta(t)\tilde{T}(t)\tilde{V}(t)}{(1+\alpha_1\tilde{T}(t))(1+\alpha_2\tilde{V}(t))} - d(t)\tilde{T}(t)$$

with $\tilde{T}^0 = \tilde{T}(l\omega) = 0, l = 1, 2, 3, \ldots$ By Lemma 1, for any $r > 0$, there exists a sufficiently large enough $T_3 > 0$, such that $\tilde{V}(t) \leq N_1 + r$ for $t > T_3$. Additionally, it is straightforward to see that $x/(1+cx) \leq x$. Then, we have the following:

$$\dot{\tilde{T}}(t) \geq \mu(t) - (\beta(t)(N_1 + r) + d(t))\,\tilde{T}(t), \quad \text{for } t \geq T_3.$$

There exists a large $\bar{l}$ such that $l\omega > T_3$ for $l > \bar{l}$. Using the comparison principle, we arrive at

$$\tilde{T}(l\omega) = e^{-\int_0^{l\omega}(\beta(u)(N_1+r)+d(u))du}\left(\tilde{T}^0 + \int_0^{l\omega}\mu(s)e^{\int_0^s(\beta(u)(N_1+r)+d(u))du}ds\right) > 0$$

for any $l > \bar{l}$. Then, we see a contradiction. Thus, $\tilde{T}^0 > 0$ and $\left(\tilde{T}^0, \tilde{E}^0, \tilde{I}^0, \tilde{V}^0\right)$ is a positive $\omega$-periodic solution of (2.1). Thus, the proof is complete.

## 7. Numerical simulation

For the numerical simulations, we consider circadian rhythms as a representative example of periodic biological processes with an approximately 24-hour cycle. To incorporate such periodic effects into system (2.1), the time-dependent parameters are modeled as harmonic functions. Specifically, we assume the following:

$$\begin{cases} \mu(t) = \mu_0 + \mu_1 \sin(\omega t), \\ \beta(t) = \beta_0 + \beta_1 \sin(\omega t), \\ d(t) = d_0 + d_1 \sin(\omega t), \end{cases}$$

where $\omega = \frac{2\pi}{24}$ corresponds to a circadian period. Such a formulation is commonly adopted in models that incorporate seasonal or circadian effects [1, 12, 16], and the use of sine functions is a convenient modeling choice. We emphasize that this choice is not restrictive, as cosine functions or other phase-shifted periodic representations could be equivalently used without affecting the qualitative dynamics or the threshold results of the model.

The constant parameter values used in the numerical simulations are summarized in Table 2. These values are chosen to be biologically plausible and to illustrate the qualitative dynamical behavior predicted by the theoretical analysis. In particular, the baseline parameters $\mu_0$, $\beta_0$, and $d_0$ represent the average rates, while the amplitudes $\mu_1$, $\beta_1$, and $d_1$ capture moderate periodic fluctuations around these averages, as commonly adopted in theoretical studies of periodic epidemics and within-host

models [25, 29, 30]. The purpose of these parameter choices is not pathogen-specific calibration, but rather to demonstrate the threshold behavior and long-term dynamics predicted by the analytical results.

**Table 2.** Fixed constants used for numerical simulation.

| Parameter | $\mu_0$ | $\beta_0$ | $d_0$ | $\mu_1$ | $\beta_1$ | $d_1$ | $\omega$ |
|---|---|---|---|---|---|---|---|
| Value | 0.1 | 0.3 | 0.01 | 0.05 | 0.1 | 0.005 | $\frac{2\pi}{24}$ |

To demonstrate the long-term dynamics of system (2.1), we examine two representative scenarios. In the first case, shown in Figure 1, where the basic reproduction ratio satisfies the condition $\mathcal{R}_0 < 1$, the approximate solution of the model (2.1) converges to the virus-free periodic trajectory $\mathcal{E}_0 = (T^*(t), 0, 0, 0)$. This outcome indicates that when $\mathcal{R}_0 < 1$, the infection dies out over time, which leads to a stable periodic state characterized by the absence of the virus. In contrast, in the second case, depicted in Figure 2, where the basic reproduction ratio satisfies $\mathcal{R}_0 > 1$, the approximate solution of the model (2.1) exhibits a different asymptotic behavior. In this scenario, the solution does not converge to the virus-free state; instead, it asymptotically approaches a periodic solution where the infection persists over time. This indicates that when $\mathcal{R}_0 > 1$, the virus maintains a presence in the population, and the system reaches a new periodic state in which the infection continues to exist. Therefore, these two cases demonstrate the critical threshold effect dictated by the value of $\mathcal{R}_0$, thereby highlighting the conditions under which the infection either dies out or persists within the host population.

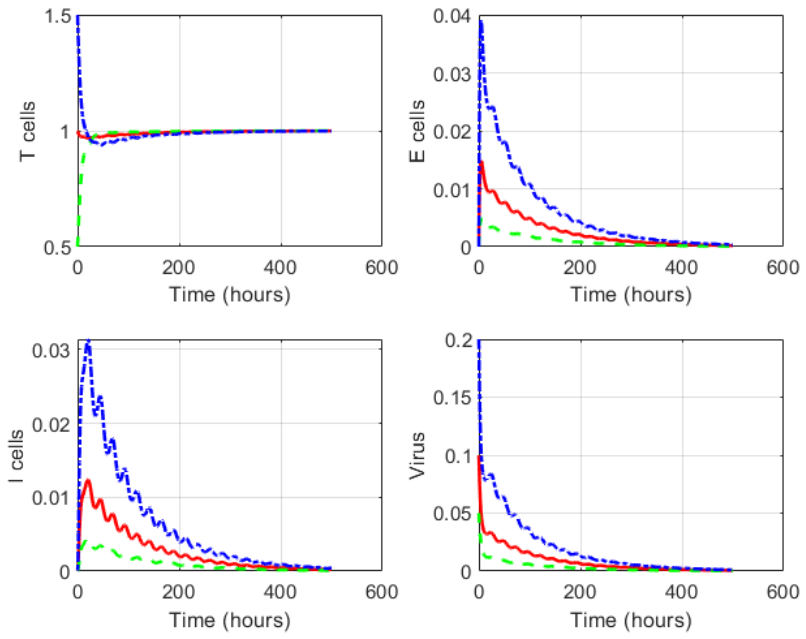


**Figure 1.** Time evolution of system (2.1) for several initial states in the regime $\mathcal{R}_0 < 1$. The trajectories for the variables $T$, $E$, $I$, and $V$ are displayed over a 10-day (240-hour) interval. The simulations use the following constant parameter values: $\alpha_1 = 0.1$, $\alpha_2 = 0.1$, $k = 0.2$, $\delta = 0.09$, $p = 0.5$, and $c = 0.18$.

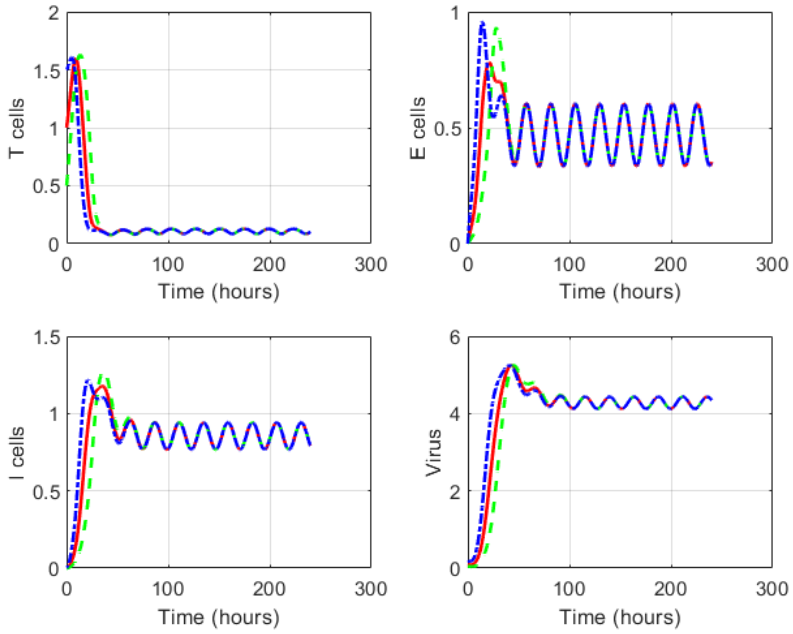


**Figure 2.** Time evolution of system (2.1) for several initial states in the regime $\mathcal{R}_0 > 1$. The trajectories for the variables $T$, $E$, $I$, and $V$ are displayed over a 10-day (240-hour) interval. The constant parameter values used here are: $\alpha_1 = 0.1$, $\alpha_2 = 0.1$, $k = 0.2$, $\delta = 0.1$, $p = 0.5$, and $c = 0.1$.

In Figure 3, we provide an enlarged view of the limit cycle that corresponds to the case where $\mathcal{R}_0 > 1$. This magnification allows for a clearer visualization of the system's dynamics when the infection persists. The figure illustrates the periodic oscillations that characterize the limit cycle behavior, thus emphasizing how the trajectories converge to a stable periodic orbit.

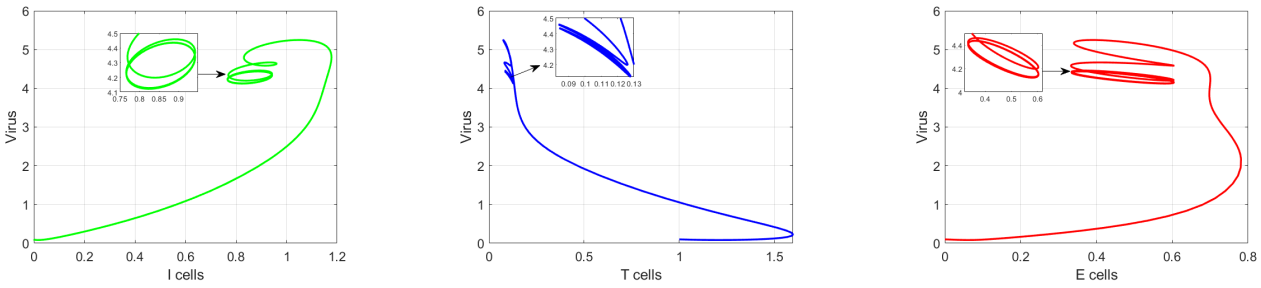


**Figure 3.** Magnified view of the limit cycle of the dynamics (2.1).

## 8. Conclusions and discussion

In this work, we proposed a within-host infection model that incorporates periodic forcing through time-dependent parameters, thus allowing the formulation to reflect biological rhythms such as circadian variations. The primary objective was to investigate the threshold behaviour of the system,

which is dictated by the basic reproduction ratio $\mathcal{R}_0$. Our analysis showed that this quantity governs the global qualitative dynamics of the infection.

When $\mathcal{R}_0 < 1$, we proved that the virus-free periodic solution $\mathcal{E}_0$ is globally asymptotically stable. Consequently, the infection is cleared regardless of the initial viral load. In contrast, in the regime $\mathcal{R}_0 > 1$, the model predicts persistence of the infection: solutions converge to a positive periodic orbit that represents a sustained viral presence within the host.

A significant aspect of our model is the incorporation of the CMFR to describe the infection rate. Unlike simpler mass-action incidence, the CMFR provides a more realistic representation of the host–pathogen interaction by accounting for saturation effects that arise from the limited availability of susceptible cells in the presence of an increasing viral load.

Our numerical simulations further support these theoretical findings. They indicate that for $\mathcal{R}_0 > 1$, there exists a unique positive periodic solution that is globally asymptotically stable. This result implies that when the reproduction number exceeds unity, the infection dynamics do not merely randomly oscillate; instead, they settle into a predictable and recurring pattern over time. This periodic behavior highlights the importance of considering time-dependent factors for the within-host models, as they can significantly affect the infection persistence and overall progression.

In conclusion, this work provides new insights into the role of periodic factors in the dynamics of within-host infection models and highlights the role of the CMFR in capturing complex biological interactions. The results demonstrate how time-dependent effects can substantially influence infection dynamics and long-term outcomes. Although the model is biologically motivated, the analysis is not restricted to a specific pathogen and applies more generally to the within-host viral infection dynamics. As a natural continuation of this study, future work will focus on integrating real-world data to refine the model, enable pathogen-specific calibration, and enhance its applicability to realistic infection scenarios.

## Author contributions

**Ibrahim Nali**: Writing – review & editing, Writing – original draft, Visualization, Validation, Software, Methodology, Investigation, Formal analysis, Conceptualization. **Attila Dénes**: Writing – review & editing, Visualization, Validation, Supervision, Software, Resources, Project administration, Methodology, Investigation, Formal analysis, Conceptualization. All authors have read and approved the final version of the manuscript for publication.

## Use of Generative-AI tools declaration

The authors declare that they have not used Artificial Intelligence (AI) tools in the creation of this article.

## Acknowledgements

This research was supported by project TKP2021-NVA-09, implemented with the support provided by the Ministry of Innovation and Technology of Hungary from the National Research, Development and Innovation Fund, financed under the TKP2021-NVA funding scheme. On behalf of the RRF-

2.3.1-21-2022-00006 project we are grateful for the possibility to use HUN-REN Cloud (see Héder et al. 2022; https://science-cloud.hu/) which helped us achieve the results published in this paper. I.N. was supported by ÚNKP-23-3-New National Excellence Program of the Ministry for Innovation and Technology from the source of the National Research, Development and Innovation Fund and Stipendium Hungaricum scholarship with Application No. 403679. A.D. was supported by the National Laboratory for Health Security, RRF-2.3.1-21-2022-00006 and by the project No. 129877, implemented with the support provided from the National Research, Development and Innovation Fund of Hungary, financed under the KKP_19 funding scheme. This publication is funded by University of Szeged Open Access Fund (grant number: 8211).

## Conflict of interest

The authors declare that they have no conflict of interest related to this research. The authors have no financial interests in any companies or organizations that could benefit from the results of this study. This research was conducted independently and without any influence from any third parties.

## References

1. H. Almuashi, Mathematical analysis for the influence of seasonality on chikungunya virus dynamics, *Int. J. Anal. Appl.*, **22** (2024), 86. https://doi.org/10.28924/2291-8639-22-2024-86
2. B. S. Alshammari, D. S. Mashat, F. O. Mallawi, Mathematical and numerical investigations for a cholera dynamics with a seasonal environment, *Int. J. Anal. Appl.*, **21** (2023), 127. https://doi.org/10.28924/2291-8639-21-2023-127
3. N. Bacaër, M. G. M. Gomes, On the final size of epidemics with seasonality, *Bull. Math. Biol.*, **71** (2009), 1954–1966. https://doi.org/10.1007/s11538-009-9433-7
4. N. Bacaër, S. Guernaoui, The epidemic threshold of vector-borne diseases with seasonality: the case of cutaneous leishmaniasis in Chichaoua, Morocco, *J. Math. Biol.*, **53** (2006), 421–436. https://doi.org/10.1007/s00285-006-0015-0
5. C. J. Browne, S. S. Pilyugin, Minimizing $\nabla_0$ for in-host virus model with periodic combination antiviral therapy, *Discrete Cont. Dyn. Syst.-Ser. B*, **21** (2016), 3315–3330. https://doi.org/10.3934/dcdsb.2016099
6. S. M. Ciupe, J. M. Heffernan, In-host modeling, *Infect. Dis. Model.*, **2** (2017), 188–202. https://doi.org/10.1016/j.idm.2017.04.002
7. C. Cosner, D. L. DeAngelis, J. S. Ault, D. B. Olson, Effects of spatial grouping on the functional response of predators, *Theor. Popul. Biol.*, **56** (1999), 65–75. https://doi.org/10.1006/tpbi.1999.1414
8. P. H. Crowley, E. K. Martin, Functional responses and interference within and between year classes of a dragonfly population, *J. N. Am. Benthol. Soc.*, **8** (1989), 211–221.
9. D. L. DeAngelis, R. A. Goldstein, R. V. O'Neill, A model for tropic interaction, *Ecology*, **56** (1975), 881–892.

10. S. Debnath, P. Majumdar, S. Sarkar, U. Ghosh, Chaotic dynamics of a tri-topic food chain model with Beddington—DeAngelis functional response in presence of fear effect, *Nonlinear Dyn.*, **106** (2021), 2621–2653. https://doi.org/10.1007/s11071-021-06896-0

11. O. Diekmann, J. A. P. Heesterbeek, J. A. J. Metz, On the definition and the computation of the basic reproduction ratio $R_0$ in models for infectious diseases in heterogeneous populations, *J. Math. Biol.*, **28** (1990), 365–382. https://doi.org/10.1007/BF00178324

12. M. El Hajji, Periodic solutions for chikungunya virus dynamics in a seasonal environment with a general incidence rate, *AIMS Math.*, **8** (2023), 24888–24913. https://doi.org/10.3934/math.20231269

13. M. El Hajji, M. F. S. Aloufi, M. H. Alharbi, Influence of seasonality on Zika virus transmission, *AIMS Math.*, **9** (2024), 19361–19384. https://doi.org/10.3934/math.2024943

14. C. P. Farrington, On vaccine efficacy and reproduction numbers, *Math. Biosci.*, **185** (2003), 89–109. https://doi.org/10.1016/s0025-5564(03)00061-0

15. S. Guerrero-Flores, O. Osuna, C. Vargas-de Leon, Periodic solutions for seasonal SIQRS models with nonlinear infection terms, *Electron. J. Differ. Equ.*, **2019** (2019), 1–13.

16. J. Gupta, J. Dhar, P. Sinha, An eco-epidemic model with seasonal variability: a non-autonomous model, *Arab. J. Math.*, **11** (2022), 521–538. https://doi.org/10.1007/s40065-022-00375-z

17. N. Heitzman-Breen, J. Golden, A. Vazquez, S. C. Kuchinsky, N. K. Duggal, S. M. Ciupe, Modeling the dynamics of Usutu virus infection in birds, *J. Theor. Biol.*, **531** (2021), 110896. https://doi.org/10.1016/j.jtbi.2021.110896

18. G. Hou, Z. Lv, W. Liu, S. Xiong, Q. Zhang, C. Li, et al., An aquatic virus exploits the IL6-STAT3-HSP90 signaling axis to promote viral entry, *PLOS Pathog.*, **19** (2023), e1011320. https://doi.org/10.1371/journal.ppat.1011320

19. M. B. Hridoy, An exploration of modeling approaches for capturing seasonal transmission in stochastic epidemic models, *Math. Biosci. Eng.*, **22** (2025), 324–354. https://doi.org/10.3934/mbe.2025013

20. K. Koelle, A. P. Farrell, C. B. Brooke, R. Ke, Within-host infectious disease models accommodating cellular coinfection, with an application to influenza, *Virus Evol.*, **5** (2019), vez018. https://doi.org/10.1093/ve/vez018

21. D. Li, W. Ma, Asymptotic properties of a HIV-1 infection model with time delay, *J. Math. Anal. Appl.*, **335** (2007), 683–691. https://doi.org/10.1016/j.jmaa.2007.02.006

22. J. Ma, Z. Ma, Epidemic threshold conditions for seasonally forced SEIR models, *Math. Biosci. Eng.*, **3** (2006), 161–172.

23. M. E. Martinez, The calendar of epidemics: seasonal cycles of infectious diseases, *PLOS Pathog.*, **14** (2018), e1007327. https://doi.org/10.1371/journal.ppat.1007327

24. G. Mazzoccoli, M. Vinciguerra, A. Carbone, A. Relógio, The circadian clock, the immune system, and viral infections: the intricate relationship between biological time and host-virus interaction, *Pathogens*, **9** (2020), 83. https://doi.org/10.3390/pathogens9020083

25. Y. Nakata, T. Kuniya, Global dynamics of a class of SEIRS epidemic models in a periodic environment, *J. Math. Anal. Appl.*, **363** (2010), 230–237. https://doi.org/10.1016/j.jmaa.2009.08.027

26. I. Nali, A. Dénes, Global dynamics of a within-host model for usutu virus, *Computation*, **11** (2023), 226. https://doi.org/10.3390/computation11110226

27. B. Paul, S. Debnath, P. Majumdar, S. Sarkar, U. Ghosh, Effect of environmental fluctuation in the dynamics of a three-species food chain model with sexually reproductive generalized type top predator and Crowley–Martin type functional response between predators, *Braz. J. Phys.*, **53** (2023), 64. https://doi.org/10.1007/s13538-023-01262-4

28. L. Perko, *Differential equations and dynamical systems*, Vol. 7, Springer Science & Business Media, 2001. https://doi.org/10.1007/978-1-4613-0003-8

29. D. Posny, J. Wang, Modelling cholera in periodic environments, *J. Biol. Dynam.*, **8** (2014), 1–19. https://doi.org/10.1080/17513758.2014.896482

30. W. Wang, X. Q. Zhao, Threshold dynamics for compartmental epidemic models in periodic environments, *J. Dyn. Differ. Equ.*, **20** (2008), 699–717. https://doi.org/10.1007/s10884-008-9111-8

31. Z. Wang, X. Q. Zhao, A within-host virus model with periodic multidrug therapy, *Bull. Math. Biol.*, **75** (2013), 543–563. https://doi.org/10.1007/s11538-013-9820-y

32. Y. Yang, Global analysis of a virus dynamics model with general incidence function and cure rate, *Abstr. Appl. Anal.*, **2014** (2014), 1–7. https://doi.org/10.1155/2014/726349

33. X. Q. Zhao, *Dynamical systems in population biology*, Springer International Publishing, 2017. https://doi.org/10.1007/978-3-319-56433-3